JACS
JOURNAL OF THE AMERICAN CHEMICAL SOCIETY
Article
pubs.acs.org/JACS

# On the Mechanism of the Initiation Reaction in Grubbs–Hoveyda Complexes

Vasco Thiel, Marina Hendann, Klaus-Jürgen Wannowius, and Herbert Plenio*

Organometallic Chemistry, FB Chemie, Petersenstr. 18, 64287 Darmstadt, TU Darmstadt, Germany

Supporting Information

**ABSTRACT:** Grubbs–Hoveyda-type complexes with variable 4-R (complexes **1**: 4-R = $NEt_2$, O*i*Pr, H, F, $NO_2$) and 5-R substituents (complexes **2**: 5-R = $NEt_2$, O*i*Pr, Me, F, $NO_2$) at the 2-isopropoxy benzylidene ether ligand and with variable 4-R substituents (complexes **3**: 4-R = H, $NO_2$) at the 2-methoxy benzylidene ether ligand were synthesized and the respective Ru(II/III) redox potentials (ranging from $\Delta E$ = +0.46 to +1.04 V), and UV–vis spectra recorded. The initiation kinetics of complexes **1**–**3** with the olefins diethyl diallyl malonate (DEDAM), butyl vinyl ether (BuVE), 1-hexene, styrene, and 3,3-dimethylbut-1-ene were investigated using UV–vis spectroscopy. Electron-withdrawing groups at the benzylidene ether ligands were found to increase the initiation rates, while electron-donating groups lead to slower precatalyst activation; accordingly with DEDAM, the complex **1**($NO_2$) initiates almost 100 times faster than **1**($NEt_2$). The 4-R substituents (para to the benzylidene carbon) were found to have a stronger influence on physical and kinetic properties of complexes **1** and **2** than that of 5-R groups para to the ether oxygen. The DEDAM-induced initiation reactions of complexes **1** and **2** are classified as two-step reactions with an element of reversibility. The hyperbolic fit of the $k_{obs}$ vs [DEDAM] plots is interpreted according to a dissociative mechanism (D). Kinetic studies employing BuVE showed that the initiation reactions simultaneously follow two different mechanistic pathways, since the $k_{obs}$ vs [olefin] plots are best fitted to $k_{obs} = k_D \cdot k_4/k_{-D} \cdot [\text{olefin}]/(1 + k_4/k_{-D} \cdot [\text{olefin}]) + k_I \cdot [\text{olefin}]$. The $k_I \cdot [\text{olefin}]$ term dominates the initiation behavior of the sterically less demanding complexes **3** and was shown to correspond to an interchange mechanism with associative mode of activation ($I_a$), leading to very fast precatalyst activation at high olefin concentrations. Equilibrium and rate constants for the reactions of complexes **1**–**3** with the bulky $PCy_3$ were determined. In general, sterically demanding olefins (DEDAM, styrene) and Grubbs–Hoveyda type complexes **1** and **2** preferentially initiate according to the dissociative pathway; for the less bulky olefins (BuVE, 1-hexene) and complexes **1** and **2** both *D* and $I_a$ are important. Activation parameters for BuVE reactions and complexes **1**($NEt_2$), **1**(H), and **1**($NO_2$) were determined, and $\Delta S^{\ddagger}$ was found to be negative ($\Delta S^{\ddagger}$ = −113 to −167 $J \cdot K^{-1} \cdot mol^{-1}$) providing additional support for the $I_a$ catalyst activation.


## INTRODUCTION

Olefin metathesis has become a powerful tool in both organic[1] and polymer synthesis.[2] It is the preferred methodology for the construction of carbon–carbon double bonds,[3] for heterocycles[4] and in total synthesis,[5] for green chemistry,[6] for protein modifications[7] or in pharmaceutical chemistry.[8] In addition to tungsten- and molybdenum-based complexes,[9] a large number of different ruthenium complexes are known to catalyze such transformations.[10] Obviously, a detailed understanding of the mechanism of olefin metathesis with such complexes is essential. Systematic mechanistic studies on the initiation reactions of Grubbs first- and second-generation (Scheme 1, A) complexes established that the dissociation of the phosphine ligand from the ruthenium center constitutes the rate-limiting step.[11] The knowledge of the initiation mechanism aided the development of fast-initiating ruthenium complexes useful for the synthesis of low-dispersity polymers (Scheme 1, B)[2a,12] or of slowly initiating complexes **C**, which are suitable for olefin metathesis reactions of sterically demanding substrates.[13] The synthesis of rapidly initiating ruthenium precatalysts (Scheme 1, D) by Piers and van der Eide[14] enabled efficient initiation reactions at low temperatures. At −50 °C ruthenacyclobutane was shown to exist as a key intermediate in olefin metathesis and was studied in detail by NMR spectroscopy.[15] More recently exhaustive low-temperature NMR experiments allowed mapping of the key steps in ring-closing metathesis reactions

**Scheme 1. Precatalysts for Olefin Metathesis Reactions**

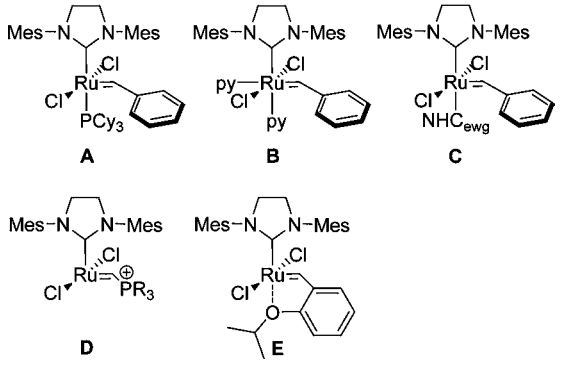


**Received:** September 23, 2011
**Published:** December 21, 2011

   dx.doi.org/10.1021/ja208967h | *J. Am. Chem.Soc.* 2012, 134, 1104–1114

and obtaining an energy profile of the initiation reaction.[25] The energy barriers along the RCM path were shown to be small, consequently the catalyst utilized has an inherent high reactivity.

In order to change the activity of a precatalyst for given olefin metathesis transformations, two approaches are useful: (a) to change the nature of the active species in the catalytic cycle by modifying the nature of the NHC ligand and (b) to adjust the initiation rate of the precatalyst. The first approach led to the development of numerous complexes with modified NHC ligands or anionic ligands other than chloride.[10b] However, approach (b), which relies primarily on changing the initiation rate of the precatalyst by varying the nature of the leaving group, can also be highly efficient, despite the fact that following the initiation reaction, this approach probably generates the same active species.[16] Both methods led to the development of a large number of new precatalysts,[17] which initiate much more rapidly[14,18] or much more slowly (latent catalysts) than precatalyst A.[19]

Hoveyda et al. and Blechert et al. reported on stable ruthenacarbenes derived from Grubbs-type complexes, in which benzylidene and $PCy_3$ are replaced by a bidentate benzylidene ether ligand (**E** in Scheme 1).[20] Such complexes do not contain phosphines, are air and moisture resistant, and have been tested successfully in numerous olefin metathesis reactions.[21] Dorta et al.[22] and Grubbs et al.[23] demonstrated that at very high olefin concentrations, Grubbs–Hoveyda-type complexes can be extremely efficient in ring closing metathesis (RCM).[24] This behavior is less easily accommodated with a purely dissociative mechanism. It was shown later that the olefin is involved in the rate-limiting step of precatalyst initiation, and consequently, high olefin concentrations lead to rapid catalyst initiation and excellent catalytic activity.[25]

A popular modification of Grubbs–Hoveyda complexes, leading to faster initiating precatalysts is the introduction of a 5-$NO_2$ group as a substituent at the benzylidene ether ligand.[18a] It is believed that the diminished electron density at the ether oxygen leads to a labile Ru–O interaction and consequently faster initiation. The effect of substituents at the benzylidene ether ligand in Grubbs–Hoveyda type complexes on the catalytic performance was studied by Blechert et al. in a systematic manner.[26] Complexes with different R groups in the 3-, 4-, or 5- position of the benzylidene ether ligand were tested in several olefin metathesis reactions. The conversion after 4.5 h and the time required to achieve 50% conversion were evaluated. The influence of substituents on substrate conversion was found to correlate with the respective $\sigma^+$- Hammett parameter of R.

Barbasiewicz and Grela et al. explained why certain structural modifications (Scheme 2) lead to faster or slower initiating

**Scheme 2. Grubbs–Hoveyda-Type Complexes with Naphthyl Groups**

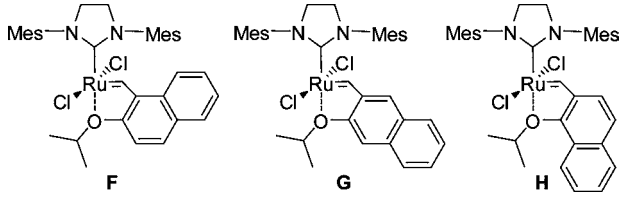


precatalysts and what the origin of this behavior is.[17b,18a,27] Specifically it was considered that there is an aromaticity-controlled activity of ruthenium metathesis catalysts.[28] A simple topological analysis of several naphthalene-based analogues of the Grubbs–Hoveyda complex, based on the Clar rule, indicated that complexes with a delocalized cyclic structure "ruthenafurane" provided (Scheme 2, F and H) provided slowly initiating complexes. The absence of a delocalized structure in the five-membered ring leads to rapidly initiating precatalysts (Scheme 2, G).

Recently a DFT study by Solans-Montfort et al. provided additional support for the relationship between the extent of delocalized structure and catalyst reactivity.[29] More specifically the catalytic activity was found to be correlated with the bond length between the carbene carbon and the $\alpha$-carbon in the phenyl ring. Based on a dissociative mechanism, no correlation between the energy of the ruthenium–oxygen interaction and catalyst activity was observed.

A different view was provided by Vougioukalakis and Grubbs who, based on negative activation entropies for the initiation reaction, suggested an associative mechanism to be operative for the initiation reaction of Grubbs–Hoveyda-type complexes.[30] In a preliminary communication we reported on conclusive evidence for the participation of the incoming olefin and the outgoing ether unit in the rate-limiting step,[25a] which led us to propose an interchange mechanism. Additional evidence had suggested that the nature of the rate-limiting step may change at high olefin concentrations.[25a] More recently Hillier, Percy et al. performed a combined experimental and quantum chemical study.[31] For the initiation reaction of Grubbs–Hoveyda-type complexes involving ethene as the olefinic substrate, an associative mechanism was proposed. In the case of sterically more demanding olefins, such as ethyl vinyl ether, an interchange mechanism provided the best fit for experimental and calculated activation parameters. The controversial results on the mechanism of the inititation reaction in Grubbs–Hoveyda type complexes prompted us to investigate this reaction in much more detail. Consequently, we wish to report here on the results of these studies.

## RESULTS AND DISCUSSION

**Synthesis of Grubbs–Hoveyda-Type Complexes.** Complexes **1** and **2** (Scheme 3) with different groups in the 4- and

**Scheme 3. Grubbs–Hoveyda-Type Complexes with Different $R^4$, $R^5$ Groups Named according to 1($R^4$), 2($R^5$), and 3($R^4$): 1($NEt_2$), 1(O*i*Pr), 1(H), 1(F), 1($NO_2$), 2($NEt_2$), 2(O*i*Pr), 2(Me), 2(F), 2($NO_2$), 3(H), and 3($NO_2$)**

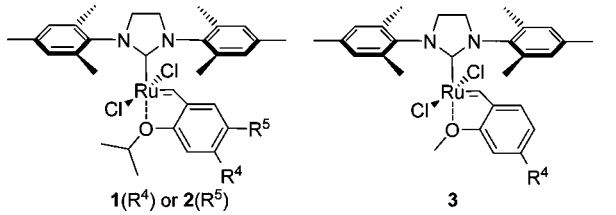


5-position of the benzylidene ether ligand were synthesized according to literature procedures.[18a,c,26,32] The 4- and 5-positions were chosen to minimize steric effects on the initiation reaction and focusing on electronic effects instead. The respective substituents were selected to cover a large range of electronic effects; several of the substituents are characterized by very different meta- and para-Hammett parameters.[33] The steric bulk of complexes **1** and **2** with 2-isopropoxy groups was modified by synthesizing closely related complex **3** with the smaller 2-methoxy ether groups. The new complexes **2**($NEt_2$) and **3**($NO_2$) were prepared according to a general procedure


dx.doi.org/10.1021/ja208967h | J. Am. Chem.Soc. 2012, 134, 1104–1114

recently reported.[34] In contrast, to all of the other complexes utilized in the present study, **3**($NO_2$) decomposes in solution. This complex is difficult to purify by chromatography and consequently **3**($NO_2$) is only obtained in ca. 25% yield.[35]

**Electrochemistry.** In order to obtain information on the electron density at the ruthenium, the Ru(II/III) redox potentials of the various complexes **1**−**3** were determined by cyclic voltammetry (Table 1). For complexes **1** the redox potentials range from +0.460 to +1.038 V and for complexes **2** from 0.678 to 1.001 V.[36] Obviously, the influence of the 4-R group on the Ru(II/III) redox potential is stronger than that of the 5-R group. Since the 4-R substituents are located para to the benzylidene carbon and meta to the ether oxygen, it is likely that the Ru(II/III) redox potentials are primarily influenced via the benzylidene carbon and to a lesser degree via the ether oxygen donor. This view is supported by the fact that there is a reasonable correlation ($R^2$ = 0.92) of the respective $\sigma$ -Hammett parameters relative the benzylidene carbon and the redox potentials of complexes **1** and **2** (Figure 1).[37] The analogous plot using Hammett constants relative to the ether oxygen is uncorrelated ($R^2$ = 0.40) (Supporting Information, SI-54).[38] Replacing an 2-isopropoxy group in complexes **1** by a 2-methoxy substituent in complexes **3** has a small influence on the Ru(II/III) redox potential.

**Table 1. Ruthenium (II/III) Redox Potentials for Complexes 1−3**[a]

| complex | redox potential (V) | $E_a - E_c$ (mV) |
|---|---|---|
| **1**($NEt_2$) | 0.460 | 78 |
| **1**(O*i*Pr) | 0.705 | 66 |
| **1**(H) | 0.837 | 63 |
| **1**(F) | 0.859 | 66 |
| **1**($NO_2$) | 1.038 | 69 |
| **2**(F) | 0.908 | 72 |
| **2**($NEt_2$) | 0.678 | 72 |
| **2**(O*i*Pr) | 0.823 | 72 |
| **2**(Me) | 0.821 | 69 |
| **2**($NO_2$) | 1.001 | 69 |
| **3**(H) | 0.886 | 77 |
| **3**($NO_2$) | 1.09 | >95 |

[a] $E_a - E_c$ is the difference between anodic and cathodic peak potential; solvent: $CH_2Cl_2$, scan rate: 100 $mVs^{-1}$, supp. electrolyte 0.1 M $NBu_4PF_6$ ref. vs $FcMe_8$ $E_{1/2}$ = +0.010 V.

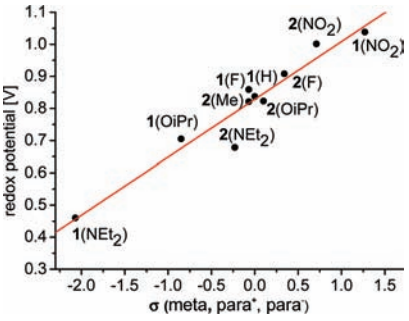


**Figure 1.** Plot of Hammett $\sigma$-parameter of the $R^4$ ($\sigma_{para+}$, $_{para-}$) and $R^5$ ($\sigma_{meta}$) group in complexes **1** and **2** relative to the benzylidene carbon.

**UV−vis Spectra.** The UV−vis spectra of complexes **1**−**3** (Figures 2 and 3) are characterized by one or two strong absorbances ($\varepsilon$ = 7000−20 000 $L{\cdot}mol^{-1}{\cdot}cm^{-1}$) between 370−500 nm (Table 2), which are likely due to metal-to-ligand charge transfer (MLCT) into the $\pi^*$ orbital of the Ru=CHR bond.[39] This MLCT band provides an excellent spectroscopic handle for monitoring the reactions of the respective Grubbs−Hoveyda-type complexes. Changes in the 4-R group lead to larger variations of $\lambda_{max}$ (374−429 nm) and $\varepsilon$ (7658−20 092 $L{\cdot}mol^{-1}{\cdot}cm^{-1}$) than with the 5-R group (370−388 nm, 6964−9043 $L{\cdot}mol^{-1}{\cdot}cm^{-1}$). The three 4-R groups which can enter into direct resonance with the ruthenium display the highest extinction coefficients. Two additional much weaker absorbances ($\varepsilon$ = 40−250 $L{\cdot}mol^{-1}{\cdot}cm^{-1}$) are observed in complexes **1**−**3** between 500−700 nm. Due their low extinction coefficients, these bands probably originate from d−d transitions.

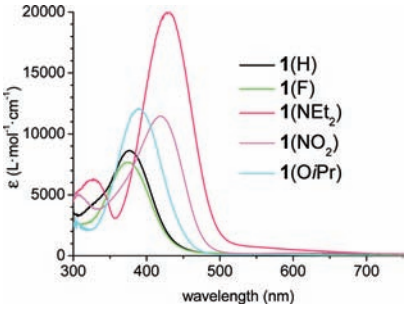


**Figure 2.** UV−vis spectra of the 4-R substituted Grubbs−Hoveyda-type complexes **1** in toluene.

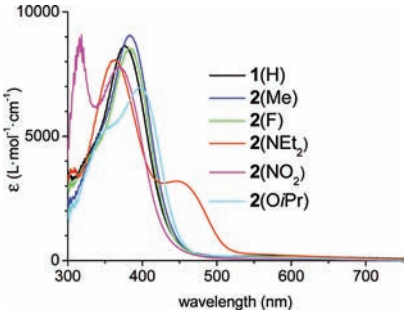


**Figure 3.** UV−vis spectra of the 5-R substituted Grubbs−Hoveyda-type complexes **2** in toluene.

**Table 2. UV−vis Data of Complexes 1−3**[a]

| complex | $\lambda_{max}$ (nm) | $\varepsilon$ ($L{\cdot}mol^{-1}{\cdot}cm^{-1}$) | $\lambda_{max}$ (nm) | $\varepsilon$ ($L{\cdot}mol^{-1}{\cdot}cm^{-1}$) |
|---|---|---|---|---|
| **1**($NEt_2$) | 429 | 20090 | 535, 639 | 250, 90 |
| **1**(O*i*Pr) | 388 | 12050 | 546, 635 | 100, 50 |
| **1**(H) | 376 | 8630 | 554, 673 | 120, 60 |
| **1**(F) | 374 | 7660 | 520, 642 | 190, 100 |
| **1**($NO_2$) | 419 | 11470 | 581, 717 | 210, 180 |
| **2**($NEt_2$) | 363, 450 | 8080, 3180 | 561, 665 | 90, 40 |
| **2**(O*i*Pr) | 398 | 6960 | 585, 683 | 120, 60 |
| **2**(Me) | 384 | 9040 | 551, 663 | 130, 90 |
| **2**(F) | 383 | 8540 | 517, 626 | 160, 80 |
| **2**($NO_2$) | 370 | 7800 | 551, 635 | 110, 70 |
| **3**(H) | 368 | 6600 | 522, 626 | 150, 80 |
| **3**($NO_2$) | 407 | 9537 | 548, 702 | 240, 150 |

[a] Spectra recorded in toluene ($10^{-4}$ M [Ru]) and 1.00 cm path length. Data for weaker absorbances obtained from Gauss fits.

**Initiation Reaction of Complex 1(H) with Diethyl Diallyl Malonate (DEDAM), Butyl Vinyl Ether (BuVE), and 1-Hexene and Discussion.** In order to obtain information


dx.doi.org/10.1021/ja208967h | J. Am. Chem.Soc. 2012, 134, 1104−1114

on the mechanism of precatalyst activation, the reactions of complex **1**(H) with the olefinic substrates DEDAM, BuVE, and 1-hexene were studied under pseudo first-order conditions ([olefin] ≫ [**1**(H)]) as a function of the substrate concentration over 2 orders of magnitude for [DEDAM] = 0.01 − 2.0 mol·L$^{-1}$, [BuVE], and [1-hexene] = 0.01−3.5 mol·L$^{-1}$ at constant [**1**(H)] = 1.0 × 10$^{-4}$ mol·L$^{-1}$ in toluene solvent at 303 K. The kinetic evaluation of precatalyst activation is based on time-dependent UV−vis spectra at the maximum of the peak at 376 nm.[40] The absorbance vs time data for the olefin initiation were fitted to a single exponential or a hyperbolic function (see Supporting Information, S28−S29) to obtain the respective $k_{obs}$ according to the kinetic model reported previously.[25a]

$$v = -\,d[Ru]/dt = k_{obs}\cdot[Ru] \quad (1)$$

The dependencies of the observed pseudo first-order rate constants $k_{obs}$ on the olefin concentrations are shown in Figure 4;[41] for all complexes a weakly curved dependence is obtained.[42]

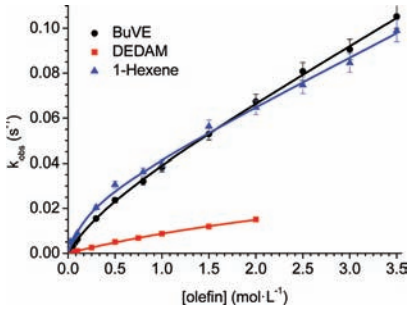


**Figure 4.** Plot of $k_{obs}$ vs [olefin] (olefin = DEDAM, BuVE, 1-hexene) for complex **1**(H).

*DEDAM.* The $k_{obs}$ vs [DEDAM] data for complex **1**(H) were successfully fitted to a hyperbolic function (eq 2).

$$k_{obs} = m_0\cdot[olefin]/(1 + b\cdot[olefin]) \quad (2)$$

The parameter $m_0$ stands for the initial slope and $b$ is a measure of the curvature. A previously employed linear function[25a,31] also provides excellent fit parameters for the present data, but the fit residuals show systematic deviations, which are apparent when a large number of data points in the appropriate concentration range are recorded.

The suitability of (eq 2) for the $k_{obs}$ vs [DEDAM] data suggest to view this initiation reaction as a two-step reaction with an element of reversibility.[43] Three different mechanistic scenarios have to be considered in this respect. The formal kinetics are outlined below (GH stands for the unactivated precatalyst, GH·olefin for a complex with coordinated olefin and ruthenium coordination number 6, and G represents a ruthenium complex with the dissociated ether oxygen with CN 4, see also Scheme 5):

(a) Associative scenario: GH + olefin ⇆ GH·olefin and GH·olefin → products
(b) Dead-end setting involving a nonproductive equilibrium: GH + olefin ⇆ GH·olefin and GH + olefin ⇆ products
(c) Dissociative scenario: GH ⇆ G and G + olefin → products.

The dead end scenario (b) is considered to be unlikely, since it is well-known that olefin metathesis product formation is enhanced in the presence of high olefin concentrations.[22,25a,30] This accelerated product formation appears implausible, when at the same time a nonproductive equilibrium is populated with excess olefin. Furthermore there is no spectroscopic evidence for a GH·olefin intermediate. This argument also applies to pathway (a), which is less likely, since within the mixing time no absorbance jump in the UV−vis spectra was observed, which was carefully checked with twin-chamber cuvettes (Supporting Information, Figure SI-42). An associative pathway can result in a sudden shift of the UV−vis absorbances at the beginning of the data collection, due to the rapid establishment of the pre-equilibrium of olefin and the respective Grubbs−Hoveyda complex. The $k_{obs}$ vs [DEDAM] data appear to reach a ceiling rate at high olefin concentrations. It is likely that this occurs when breaking of the ether oxygen to ruthenium bond becomes rate limiting. At this point of the discussion, a dissociative mechanism for the initiation of complexes **1**(H) appears to be the most likely choice. Later more arguments will be presented, which further support this view. We note that this explanation is compatible with the mechanism established by Sanford, Grubbs, et al. for Grubbs II type complexes.[11a] However, at this stage of the discussion, there appears to be an inconsistency with the mechanistic models proposed by Vougioukalakis and Grubbs,[30] Percy and Hillier et al.,[31] and us.[25a] Obviously additional detailed studies are required to resolve this.

*BuVE and 1-Hexene.* The two additional olefins studied in the precatalyst activation of complex **1**(H) provide different $k_{obs}$ vs [olefin] plots. Unlike the $k_{obs}$ vs [DEDAM] plot, the $k_{obs}$ vs [BuVE] or [1-hexene] data for complex **1**(H) in Figure 4 cannot be fitted satisfactorily with (eq 2), since the curve segment at concentrations higher than ca. 0.3 M [BuVE] is linear and depends on the olefin concentration. An excellent fit of the data is obtained when the hyperbolic function (eq 2) is extended with an additional linear term, with a first-order dependence on the [olefin]:

$$k_{obs} = m_0\cdot[olefin]/(1 + b\cdot[olefin]) + m_1[olefin] \quad (3)$$

In order to illustrate the individual contributions of the linear and the hyperbolic terms for the $k_{obs}$ vs [BuVE] data, both constituting terms are plotted in Figure 5. The red curve

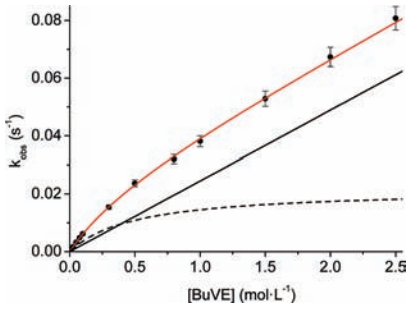


**Figure 5.** Fit of $k_{obs}$ vs [BuVE] plot according to (eq 3, red curve) for complex **1**(H) displayed in the range [BuVE] = 0−2.55 mol·L$^{-1}$ ($k_{obs}$ measured up to [BUVE] = 3.5 mol·L$^{-1}$). The contribution of eq 2 (dashed line) and $m_1$·[BuVE] (solid line) is shown.

according to (eq 3) comprises the sum of the linear and the hyperbolic curves, the dashed black line represents the contribution of the hyperbolic term in (eq 3), and the solid line stands for the linear term in (eq 3). The linear segment is the major contributor to the red curve at olefin concentrations


dx.doi.org/10.1021/ja208967h | J. Am. Chem.Soc. 2012, 134, 1104−1114

>0.5 M. Based on this extended model for the initiation of complex **1**(H) with BuVE or 1-hexene using a hyperbolic and a linear term, the initiation reactions with BuVE and 1-hexene cannot follow a simple dissociative mechanism. The use of a fit function with two additive terms implies that the initiation reaction must simultaneously follow two parallel mechanistic pathways.

**Initiation Reaction of Complexes 1−3 with BuVE and 1-Hexene.** In order to learn whether the two potential modes of precatalyst activation are general features of such complexes, a much more detailed investigation of the initiation behavior, employing 12 different complexes **1**($NEt_2$), **1**(O*i*Pr), **1**(H), **1**(F), and **1**($NO_2$); **2**($NEt_2$), **2**(O*i*Pr), **2**(Me), **2**(F), and **2**($NO_2$); and **3**(H) and **3**($NO_2$), was done. The initiation reactions with BuVE and 1-hexene were studied at 15 different olefin concentrations in the range of 0.01−3.5 mol·$L^{-1}$ under conditions similar to those reported for complex **1**(H). The respective plots of $k_{obs}$ vs [BuVE] for the Grubbs−Hoveyda complexes **1** and **3** are shown in Figure 6, those of complexes **2** in Figure 7, and the $k_{obs}$ vs [1-hexene] in the Supporting Information, Figure SI-45. The same basic features are found for all $k_{obs}$ vs [BuVE] plots of complexes **1** and **2** (Figures 6 and 7): (i) the $k_{obs}$ vs [BuVE] curve is almost

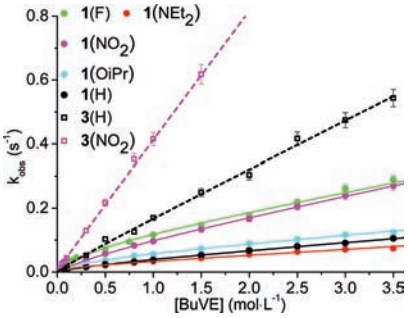


**Figure 6.** Plot of $k_{obs}$ vs [BuVE] for the four-substituted complexes **1** and **3**.

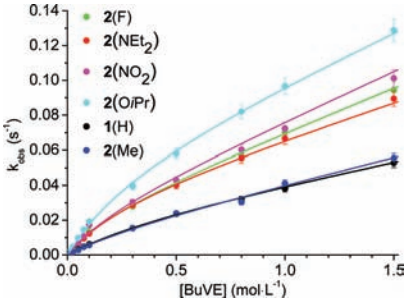


**Figure 7.** Plot of $k_{obs}$ vs [BuVE] (display range 0−1.5 mol·$L^{-1}$, data range 0.01−3.5 mol·$L^{-1}$) for the five-substituted complexes **2**.

linear at [BuVE] > 0.3−0.5 mol·$L^{-1}$, and there is a nearly linear segment with a different slope at [BuVE] < 0.3 M. Consequently, eq 3 provides excellent fits for the plots of all complexes **1** and **2**. (ii) On decreasing the bulk of the 2-alkoxy group from 2-isopropoxy to 2-methoxy in complex **3**, a pronounced increase in the rate of the initiation reaction is observed, and the $k_{obs}$ vs [olefin] plot is best fitted with $k_{obs} = m_1$[olefin].

Precatalyst activation for complexes **3** is much faster than for complexes **1** and **2** (Figure 6) and at [BuVE] = 2.5 mol·$L^{-1}$ complex **3**(H) displays a 5-fold increase of $k_{obs}$ with respect to **1**(H). Complex **3**($NO_2$) shows a 12-fold increase of $k_{obs}$ compared to **1**(H) and a 5-fold increase with respect to **1**($NO_2$). The most electron-withdrawing groups (4-F and 4-$NO_2$) lead to the most rapidly initiating complexes **1**, while the most strongly donating group (4-$NEt_2$) is the slowest. In the five-substituted complexes **2** (Figure 7), the substituents effects on $k_{obs}$ are not according to the electron-donating capacity with respect to the para-position. Instead the 5-O*i*Pr substituent, which is electron donating with respect to the para-position but electron-withdrawing with respect to the meta-position, shows faster initiation than **2**($NO_2$). The same explanation applies to the relatively fast initiation of **2**($NEt_2$).

The $k_{obs}$ vs [1-hexene] plots for complexes **1**($NO_2$), **1**($NEt_2$), and **1**(H) (Supporting Information, Figure SI-45) are best fitted with the hyperbolic + linear function (eq 3). Again with the sterically less demanding precatalysts **3**(H) and **3**($NO_2$), a linear fit is more suitable than (eq 3).

**Initiation Reaction of Complexes 1−3 with DEDAM, Styrene, and Neohexene.** *DEDAM.* The precatalyst activation of the complexes **1**($NEt_2$), **1**(O*i*Pr), **1**(H), **1**(F), and **1**($NO_2$) and of **2**($NEt_2$), **2**(O*i*Pr), **2**(Me), **2**(F), and **2**($NO_2$), and **3**(H) and **3**($NO_2$) with DEDAM was studied under the conditions reported for **1**(H). The dependencies of the observed pseudofirst-order rate constants $k_{obs}$ on the olefin concentrations are shown in Figure 8 for the series of complexes **1** and **3** and in Figure 9 for complexes **2**. In order to better

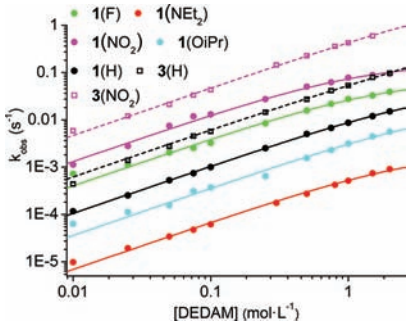


**Figure 8.** Plot (log−log) of $k_{obs}$ vs [DEDAM] for the four-substituted complexes **1** and **3**.

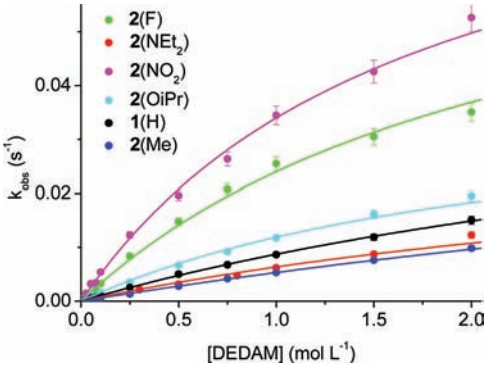


**Figure 9.** Plot of $k_{obs}$ vs [DEDAM] for the five-substituted complexes **2**.

display the large differences in $k_{obs}$ for complexes **1** and **3**, a double logarithmic representation of the data was chosen. The data in Figures 8 and 9 were fitted to $k_{obs} = m_0 \cdot$[DEDAM]/(1 + $b \cdot$[DEDAM]) (eq 2). Again the 2-methoxy-substituted complexes **3** initiate much faster than all other 2-isopropoxy complexes **1** and **2**; at [DEDAM] = 1.0 mol·$L^{-1}$, there is a 6-fold increase in $k_{obs}$ with **3**($NO_2$) compared to **1**($NO_2$). This


dx.doi.org/10.1021/ja208967h | *J. Am. Chem.Soc.* 2012, 134, 1104−1114

rate acceleration is even more pronounced at higher [BuVE] concentration when the curve for **1**($NO_2$) is almost flat, while that of **3**($NO_2$) still increases. The range of initiation rates covered by the various Grubbs–Hoveyda-type complexes is impressive: **3**($NO_2$) is ca. 1000 times faster than the slowest complex **1**($NEt_2$).

The respective $k_{obs}$ vs [DEDAM] plots of the four-substituted complexes **1** (Figure 8) are ordered along their electron-donating capacity. **1**($NEt_2$) is an extremely slowly initiating complex, being almost 100 times slower than **1**($NO_2$). For the series of complexes **2** (Figure 9) with variable 5-R substituents the spread in the initiation rates is much smaller than for complexes **1**. The weaker influence of the 5-R substituents was observed before for other physical parameters (redox potentials: Table 1; UV–vis spectra: Table 2) and appears to be typical. There seems to be a (weak) meta-effect, since **2**(O*i*Pr) and **5**($NEt_2$) are slightly faster than expected based on their respective para-donation.

*Styrene.* The initiation reactions of styrene are instructive, since this olefin appears to be a borderline case concerning the dominant mechanism of precatalyst activation. This is visible in the double logarithmic representation of the $k_{obs}$ vs [styrene] plot (Figure 10). Complexes **1**(H) and **1**($NO_2$) appear to

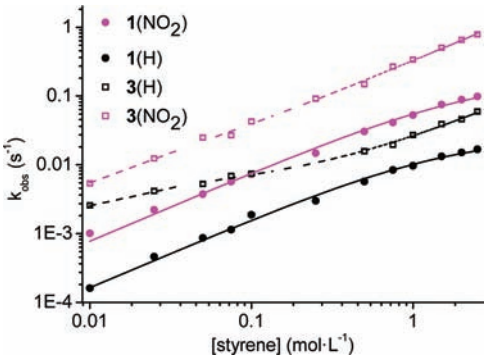


**Figure 10.** Double logarithmic plot of $k_{obs}$ vs [styrene] for the four-substituted complexes **1** and **3**.

follow a primarily dissociative initiation reaction. At high olefin concentration the contribution of the $m_1$·[styrene] term for the two complexes increases significantly relative to the hyperbolic term, and this leads to a significant bending of the fit curve. Such bent curve segments at intermediate styrene concentrations of ca. 0.02 − 0.3 mol·$L^{-1}$ denote roughly equal contributions of the two different mechanistic pathways for precatalyst initiation. For complex **3**(H) the bent curve segment is followed by another nearly linear section at styrene concentrations in excess of 0.7 mol·$L^{-1}$ and a dominant $m_1$·[styrene] term. Obviously, the main mode of precatalyst activation appears to change going from low to high styrene concentrations. For **3**($NO_2$) the dissociative initiation mechanism appears to be less important, and the linear $m_1$·[styrene] term is dominant at all styrene concentrations studied.

*Neohexene.* The precatalyst activation of **1**(H), **1**($NO_2$), and **3**(H) with a sterically very demanding olefin was also tested. As expected, the initiation reactions involving neohexene turn out to be extremely slow; roughly 1000 times slower than for 1-hexene at the same olefin concentration. The $k_{obs}$ were determined at two neohexene concentrations (3.0 and 3.5 mol·$L^{-1}$) and found to be: **1**($NO_2$) 2.1 ·$10^{-4}$ $s^{-1}$ (3.5 mol·$L^{-1}$) and 1.9 ·$10^{-4}$ $s^{-1}$ (3.0 mol·$L^{-1}$); **1**(H) 2.4 ·$10^{-5}$ $s^{-1}$ (3.5 mol·$L^{-1}$) and 1.4 ·$10^{-5}$ $s^{-1}$ (3.0 mol·$L^{-1}$); **3**(H) 9.6 ·$10^{-5}$ $s^{-1}$ (3.5 mol·$L^{-1}$) and 8.6 × $10^{-5}$ $s^{-1}$ (3.0 mol·$L^{-1}$). Complex **1**($NO_2$) undergoes faster precatalyst activation than **1**(H) and **3**(H). This is suggestive of a primarily dissociative mode of activation.

**Reaction of Grubbs–Hoveyda Complexes 1–3 with $PCy_3$.** This reaction leads to the substitution of the oxygen donor by the phosphine ligand (Scheme 4) and might serve as

**Scheme 4. Reaction of Grubbs–Hoveyda Complex with $PCy_3$**

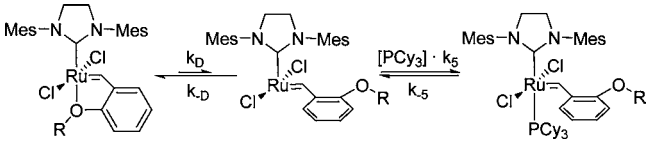


a simple model for the first steps of the initiation reaction. The structure of the $PCy_3$ addition product in solution was previously confirmed by nuclear Overhauser enhancement spectroscopy experiments.[25a] With a view to the bulk of $PCy_3$, this reaction could primarily occur via a dissociative mechanism. In case this is true, the rates for the dissociation reaction of the ruthenium complexes with $PCy_3$ and olefins should be comparable. The respective equilibrium constants $K_{NMR}$ with the complexes **1–3** were determined via $^1$H NMR spectroscopy. The rate constants $k_D$ were obtained via UV–vis experiments (Table 3 and Supporting Information, Figure SI-52).

**Table 3. Kinetic and Thermodynamic Parameters for the Reaction of Complexes 1–3 with $PCy_3$ in Toluene at 303 K**

| | $K_{NMR}$ ($M^{-1}$)[a] | $k_D \cdot 10^3$ ($s^{-1}$)[b] | $k_5 \cdot k_{-D} = k_D / K_{NMR} \cdot 10^3$ (mol·$L^{-1}$·s) | $k_5 \cdot K_D \cdot 10^3$ (L·$mol^{-1}$·$s^{-1}$)[b] |
|---|---|---|---|---|
| **1**($NEt_2$) | 119 | 13.1 ± 0.8 | 0.110 | 68 ± 6 |
| **1**(O*i*Pr) | 285 | 42 ± 8 | 0.146 | 71 ± 5 |
| **1**(H) | 92 | 29.2 ± 3.3 | 0.317 | 50.5 ± 2 |
| **1**(F) | 720 | 66 ± 10 | 0.091 | 147 ± 14 |
| **1**($NO_2$) | 926 | 158 ± 32 | 0.170 | 171 ± 5 |
| **2**($NEt_2$) | 97 | 18 ± 8 | 0.188 | 40 ± 5 |
| **2**(O*i*Pr) | 180 | –[c] | –[c] | –[c] |
| **2**(Me) | 106 | 32 ± 7 | 0.306 | 76 ± 4 |
| **2**(F) | 194 | 37 ± 10 | 0.189 | 72 ± 5 |
| **2**($NO_2$) | 516 | 39 ± 30 | 0.076 | 39 ± 4 |
| **3**(H) | 88 | 156 ± 6 | 1.8 | 59 ± 24 |
| **3**($NO_2$) | 928 | 587 ± 43 | 0.63 | 70 ± 18 |

[a]Determined via the ratio of the integrals of the benzylidene protons in the $^1$H NMR spectrum, the estimated error of $K_{NMR}$ is 10%. [b]Determined via UV–vis experiments fitted to (eq 4) with olefin = $PCy_3$. [c]Spectral changes too small for evaluation.

The ordering of the equilibrium constants $K_{NMR}$ and of $k_D$ is roughly according to the electron-donating abilities. Again the interpretation of the substituent effects is not straightforward, since the coordinating properties of ruthenium and of the ether oxygen can be influenced via a combination of meta- and para-effects of the 4- and 5-substituents. The rate constants $k_D$ obtained from the $PCy_3$ substitution reactions and from the BuVE or the 1-hexene experiments for the respective complexes **1** and **2** show good agreement (see Table 4) for the data in the concentration range ([$PCy_3$] = 0.001–0.3 mol·$L^{-1}$).[44] For the reactions of **3**(H) and **3**($NO_2$) with $PCy_3$ a significant increase


dx.doi.org/10.1021/ja208967h | J. Am. Chem.Soc. 2012, 134, 1104–1114

**Table 4. Kinetic Parameters for the Initiation Reaction of Complexes 1−3 with BuVE and 1-Hexene in Toluene at 303 K**

| | $k_D \cdot 10^3$ ($s^{-1}$) | $k_4 \cdot K_D \cdot 10^3$ ($L \cdot mol^{-1} \cdot s^{-1}$) | $k_I \cdot 10^3$ ($L \cdot mol^{-1} \cdot s^{-1}$) |
|---|---|---|---|
| BuVE | | | |
| **1**($NEt_2$) | 17.5 ± 1.3 | 109 ± 18 | 18.0 ± 0.7 |
| **1**(O*i*Pr) | 45 ± 4 | 107 ± 18 | 25.1 ± 1.4 |
| **1**(H) | 22 ± 2 | 43 ± 9 | 24.5 ± 0.8 |
| **1**(F) | 83 ± 21 | 210 ± 106 | 58 ± 8 |
| **1**($NO_2$) | 59 ± 19 | 84 ± 51 | 63 ± 6 |
| **2**($NEt_2$) | 33 ± 3 | 113 ± 22 | 39.8 ± 1.5 |
| **2**(O*i*Pr) | 54 ± 8 | 155 ± 48 | 55.5 ± 3.5 |
| **2**(Me) | 13 ± 4 | 35 ± 24 | 30 ± 2 |
| **2**(F) | 24 ± 3 | 109 ± 34 | 49.6 ± 2 |
| **2**($NO_2$) | 25 ± 9 | 102 ± 75 | 56 ± 5 |
| **3**(H) | 21 ± 18 | 61 ± 10 | 151 ± 9 |
| | | | 169 ± 5[a] |
| **3**($NO_2$) | –[c] | –[c] | 402 ± 4[a] |
| 1-Hexene | | | |
| **1**($NEt_2$) | – | 3 ± 0.05[b] | – |
| **1**(H) | 25 ± 8 | 105 ± 76 | 21 ± 4 |
| **1**($NO_2$) | 110 ± 27 | 210 ± 100 | 43 ± 9 |
| **3**(H) | –[c] | –[c] | 102 ± 4[a] |
| **3**($NO_2$) | –[c] | –[c] | 431 ± 69[a] |

[a]Obtained from linear fit $k_I \cdot$[BuVE] or $k_I \cdot$[1-hexene]. [b]Obtained from linear fit $m_1 \cdot$[1-hexene], it is not clear whether this an D or an I rate. The errors given are the errors of the fit procedure. [c]Predominant $I_a$ mechanism, $k_D$ cannot be determined.

in the substitution rates is observed relative to those of complexes **1**(H) and **1**($NO_2$). This observation is not compatible with an exclusively dissociative mechanism for the ligand substitution reaction for these complexes, while the equilibrium constants $K_{NMR}$ are the same for the related complexes **1** and **3**

**Monitoring the Rate of Styrene Release.** Two of the styrenes (4-nitro-2-isopropoxystyrene and 4-$NMe_2$-2-isopropoxystyrene) used for this study are characterized by UV−vis spectra with absorption maxima significantly different from those of the respective Grubbs−Hoveyda complexes **1**($NO_2$) and **1**($NEt_2$). Consequently, the amount of liberated styrene during olefin metathesis as well as the kinetics of this reaction can be easily monitored independent from changes occurring at the respective precatalysts. The absorbance vs time curves for the DEDAM initiation of **1**($NO_2$) were simultaneously determined at 303 K by monitoring the decay of the LMCT band at 419 nm and the increase in the styrene band at 360 nm. The respective $k_{obs}$ vs [DEDAM] plots provide nearly identical rate constants. It can thus be concluded that all steps following this first step in the initiation reaction are much faster. This also holds true when the same kinetic experiments are performed at 253 K. Despite the low temperatures, the initiation is still fast enough at high olefin concentrations to be monitored conveniently. Even at such low temperatures, the disappearance of the precatalyst band and the increase in the styrene absorbance follow almost the same rate, even though small differences begin to show up. After the initiation reaction, the concentration of liberated styrene remains constant throughout the metathesis reaction. Consequently, there is no evidence for a return of the benzylidene ligand to the ruthenium.[25b]

**Discussion of the Mechanism of Precatalyst Activation in Complexes 1−3.** Depending on the nature of the precatalysts and of the olefins, the respective $k_{obs}$ vs [olefin] plots can either be fitted with a hyperbolic function based on (eq 2), a hyperbolic + linear function $k_{obs} = m_0 \cdot$[olefin]/(1 + $b \cdot$[olefin]) + $m_1$[olefin] (eq 3) or a linear function through the origin. This has important implications for the mechanism of such reactions, which need to be discussed in detail. An outline of the potential associative, interchange, and dissociative pathways as well as the terminology of the rate constants is given in Scheme 5. Earlier in this manuscript, the hyperbolic

**Scheme 5. Reaction Scheme and Potential Intermediates in the Initiation Reaction of Grubbs−Hoveyda Complexes via Associative, Interchange, and Dissociative Pathway**

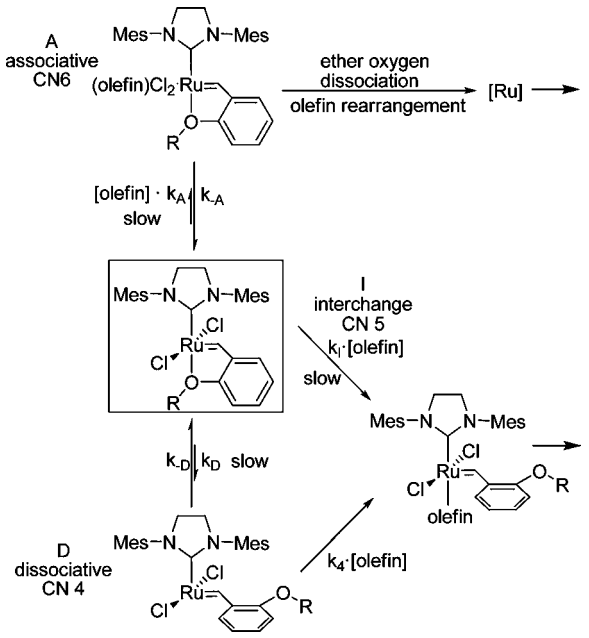


term was assigned to a dissociative pathway; based on this, eq 2 should be rewritten:

$$k_{obs} = k_D \cdot k_4 / k_{-D} \cdot [\text{olefin}] / (1 + k_4 / k_{-D} \cdot [\text{olefin}]) \quad (4)$$

Based on the applicability of eq 3, it was concluded that precatalyst activation occurs according to two parallel mechanistic pathways and that there are certain combinations of olefin and ruthenium complexes, in which one of the two possible modes of activation prevails. The respective $k_{obs}$ vs [olefin] plots for the activation of precatalysts **1** and **2** with sterically demanding substrates (DEDAM, styrene) are best fitted with (eq 4). For the reactions of smaller substrates (1-BuVE, 1-hexene) with small precatalysts **3**, a $k_{obs} = m_1 \cdot$[olefin] applies. For reactions of bulky olefins and small precatalysts **3** the same relationship appears to be the best approach in the majority of reactions, while for small olefins and complexes **1** or **2** eq 4 + $m_1$[olefin] applies.

This information serves as a starting point for the following discussion on the interpretation of the $m_1 \cdot$[olefin] term. The first-order behavior with respect to olefin and the pronounced influence of steric bulk at the olefin and the ruthenium complexes on the rates suggest that this step can either correspond to an associative or an interchange pathway for the initiation reaction (Figure 4). Those two steps cannot be differentiated kinetically with certainty for the reactions studied. However, an associative mechanism for precatalyst activation in Grubbs II complexes appears to be less likely, even though this


dx.doi.org/10.1021/ja208967h | J. Am. Chem.Soc. 2012, 134, 1104−1114

has been considered for Grubbs I complexes.[45] Our decision is based on the following arguments: DFT studies by Solans-Montfort et al. could not locate an energetically acceptable transition structure according to an associative mechanism.[29b] Related computational studies by Hillier and Percy et al. suggest an interchange mechanism for olefins other than ethene, rather than the formation of an intermediate with increased coordination number.[31] In our previous studies we had also noted the contribution of both reaction partners in the initiation process, which had led us to propose an interchange mechanism with associative mode of activation. Furthermore an associative pathway requires a six-coordinate intermediate. There are only a few solid-state structures with six-coordinate ruthenium in closely related $(NHC)RuCl_2(=CHR)$ complexes,[46] which are formed with small substrates (pyridine) or chelating ligands. An olefin bound to ruthenium in a potential intermediate with coordination number 6 will be sterically more demanding than for example a pyridine ligand, regardless of whether the olefin adds trans[45] or cis to the benzylidene.[47] Another less appealing feature of an associative pathway is that it does not seem to lead to an intermediate, which is able to directly enter the catalytic cycle.[48] Apart from the obligatory ether oxygen dissociation, an additional olefin rearrangement seems to be required.[49]

A different interpretation of the linear segment in the $k_{obs}$ vs [olefin] plots for BuVE initiation also has to be discussed. Linearity can also be observed with a purely dissociative mechanism, far from the saturation kinetics in the initial linear segment of the hyperbola controlled by $k_4 \cdot K_D$. However, we consider this alternative as unlikely. As mentioned before, it is well-known that reduced steric bulk at the catalyst favors an interchange over a dissociative pathway. Along the same line, reduced bulk at the olefinic substrate should also favor the interchange over the dissociative pathway. Finally the activation entropy, which was found to be strongly negative (see Determination of Activation Parameters for BuVE), clearly favors the I over the D pathway. Based on these arguments, the linearity of the $k_{obs}$ vs [olefin] plots is unlikely to be the result of a dissociative pathway.

Based on the results reported here, we propose an interchange mechanism with associative mode of activation ($I_a$) to account for the linear term $m_1 \cdot$[olefin] and a dissociative mechanism to account for the hyperbolic term. Such a changeover from a dissociative mechanism to a mechanism with associative character is not unusual and has been observed for various platinum and ruthenium complexes.[50] The validity of the arguments presented above will be further elaborated in the following evaluation of the rate constants obtained, according to this mechanistic model.

**Discussion of the Kinetic Parameter for BuVE and 1-Hexene Initiation.** The kinetic parameters for the BuVE induced precatalyst activation of complexes **1**−**3** were calculated by fitting the $k_{obs}$ vs [BuVE] data according to eq 4 + $k_I$[BuVE] or eq 4 + $k_I$[1-hexene] (Table 4). The interchange rate $k_I$ is the slope of the linear segment at high olefin concentrations and can be obtained from the fits with good precision. The data in Table 4 show that the rate of the interchange pathway is accelerated in complexes with electron-withdrawing groups. This is reflected in a good correlation of the Hammett parameters and $k_I$ (Supporting Information, Figure SI-56). The established view within the framework of a dissociative mechanism is that decreasing the electron density at the ether oxygen accelerates Ru−O dissociation. The results presented show that electron-withdrawing groups render an electron-deficient ruthenium, which is more willing to accept an (electron rich) olefin in an interchange pathway than an electron-rich ruthenium. Thus we note an interesting dichotomy: Rapidly initiating precatalysts are characterized by an electron-deficient ruthenium center, while the ruthenium in the catalytically active species ought to be electron rich, as claimed by Straub.[51] According to Jensen et al., an electron-rich ruthenium also increases the stability of the high oxidation state ruthenacyclobutane.[52]

The substituent-dependent variations of the rate constants $k_I$ and $k_D$ are much less pronounced in the series of complexes **2** than in complexes **1**. This phenomenon was observed before. Again there appears to be a meta-effect, since an increase in $k_I$ is also observed for **2**(O*i*Pr), whose 5-O*i*Pr substituent is electron withdrawing with respect to the meta-position.

In order to provide additional evidence for our interpretation of a simultaneous interchange and dissociative pathway for the initiation reactions utilizing Grubbs−Hoveyda complexes, the effect of a structural modification in the Grubbs−Hoveyda complexes was tested. For a given substrate the interchange pathway is expected to be more favorable with less bulky ruthenium precatalysts. Thus replacing the 2-isopropoxy group by the much smaller 2-methoxy group should favor the interchange over the dissociative pathway. Only a few such complexes have been reported in the literature, and consequently, their reactivity was rarely studied.[27d,53] The $k_{obs}$ vs [BuVE] plots for the reactions of complexes **3**(H) and **3**($NO_2$) are characterized by a very modest curvature and are almost linear over the whole concentration range. For such complexes the parameters defining the hyperbola cannot be determined reliably, and a $k_{obs} = k_I \cdot$[BuVE] fit is more appropriate. Consequently, for complexes **3** there is a strong increase in $k_I$(**3**(H)) = 0.151 $L \cdot mol^{-1} \cdot s^{-1}$ compared to $k_I$(**1**(H))= 0.0245 $L \cdot mol^{-1} \cdot s^{-1}$ and $k_I$(**3**($NO_2$))= 0.402 $L \cdot mol^{-1} \cdot s^{-1}$ compared to $k_I$(**1**($NO_2$))= 0.063 $L \cdot mol^{-1} \cdot s^{-1}$. This accelerated interchange pathway is easily explained by the reduced steric bulk of complexes **3** compared to that of complexes **1**.

The kinetic parameters of 1-hexene are comparable to those of BuVE, the most important information being the pronounced increase in the interchange rate $k_I$ on replacing the 2-isopropoxy by a 2-methoxy group in complexes **3**.

**Determination of Activation Parameters for BuVE.** In an attempt to provide additional evidence for an interchange pathway, the respective activation parameters for the initiation reactions of complexes **1**(H), **1**($NEt_2$), and **1**($NO_2$) with BuVE were determined (Table 5) by plotting the respective $k_I$ values in an Eyring plot. The $\Delta H^{\ddagger}$ ($k_I$) value for **1**(H) thus obtained is close to the value determined previously.[30] The three activation entropies derived from $k_I$ are strongly negative (−113 to −168 $J \cdot K^{-1} \cdot mol^{-1}$), which clearly points to an interchange (or an associative) initiation mechanism. The activation entropies for a dissociative mechanism are not meaningful; the opening or closing of the chelate ring in Grubbs−Hoveyda complexes does not change the number of molecules.[54]

**Discussion of the Kinetic Parameters for DEDAM and Styrene Initiation.** The $k_{obs}$ vs [DEDAM] plots can be fitted according to eq 4, and the data obtained via this approach are given in Table 6. The excellent fit parameters of the hyperbolic fit suggest that initiation reactions of complexes **1** and **2** with DEDAM operate via a dissociative mechanism. Given the higher steric demand of DEDAM as compared to BuVE, this is


dx.doi.org/10.1021/ja208967h | J. Am. Chem.Soc. 2012, 134, 1104−1114

Table 5. Activation Parameters for the Initiation of Complexes 1(H), 1($NEt_2$), and 1($NO_2$) with BuVE

| | $\Delta S^{\ddagger}$ ($k_4 \cdot K_D$) [J·K$^{-1}$·mol$^{-1}$] | $\Delta S^{\ddagger}$ ($k_I$) [J·K$^{-1}$·mol$^{-1}$] | $\Delta H^{\ddagger}$ ($k_D$) [kJ·mol$^{-1}$] | $\Delta H^{\ddagger}$ ($k_4 \cdot K_D$) [kJ·mol$^{-1}$] | $\Delta H^{\ddagger}$ ($k_I$) [kJ·mol$^{-1}$] | $\Delta G^{\ddagger}_{293K}$ ($k_4 \cdot K_D$) [kJ·mol$^{-1}$] | $\Delta G^{\ddagger}_{293K}$ ($k_I$) [kJ·mol$^{-1}$] |
|---|---|---|---|---|---|---|---|
| 1(H) | −86 ± 8 | −130 ± 26 | 67 ± 6.3 | 56 ± 3 | 43 ± 3.6 | 81 ± 4 | 82 ± 7 |
| 1($NEt_2$) | −110 ± 15 | −170 ± 81 | 68 ± 5.5 | 47 ± 3.7 | 34 ± 4.2 | 79 ± 6 | 83 ± 10 |
| 1($NO_2$) | −140 ± 37 | −110 ± 25 | 79 ± 8.7 | 38 ± 4.4 | 46 ± 5.3 | 79 ± 9 | 79 ± 9 |

Table 6. Kinetic Parameters for the Initiation Reaction of Complexes 1−3 with DEDAM and Styrene in toluene at 303 K

| | $k_4/k_{-D}\cdot10^3$ (L·mol$^{-1}$)[a] | $k_4\cdot K_D\cdot10^3$ (L·mol$^{-1}$·s$^{-1}$)[a] | $k_D\cdot10^3$ (s$^{-1}$)[a] | $k_I\cdot10^3$ (L·mol$^{-1}$·s$^{-1}$) |
|---|---|---|---|---|
| DEDAM | | | | |
| 1($NEt_2$) | 312 ± 94 | 0.69 ± 0.04 | 2.2 ± 0.5 | −[d] |
| 1(O*i*Pr) | 178 ± 138 | 3.6 ± 0.3 | 20 ± 14 | −[d] |
| 1(H) | 207 ± 29 | 10.5 ± 0.2 | 51 ± 6 | −[d] |
| 1(F) | 551 ± 165 | 40.3 ± 3.2 | 73 ± 18 | −[d] |
| 1($NO_2$) | 806 ± 134 | 132.2 ± 7.2 | 164 ± 20 | −[d] |
| 2($NEt_2$) | 218 ± 55 | 7.7 ± 0.3 | 35 ± 8 | −[d] |
| 2(O*i*Pr) | 423 ± 180 | 16.9 ± 1.6 | 40 ± 14 | −[d] |
| 2(Me) | 113 ± 61 | 5.9 ± 0.3 | 52 ± 27 | −[d] |
| 2(F) | 430 ± 97 | 34.3 ± 1.8 | 80 ± 15 | −[d] |
| 2($NO_2$) | 576 ± 93 | 53.6 ± 2.3 | 93 ± 12 | −[d] |
| 3(H) | −[d] | −[d] | −[d] | 51 ± 1[b] |
| 3($NO_2$) | −[d] | −[d] | −[d] | 416 ± 8[b] |
| Styrene | | | | |
| 1(H) | 630 ± 90 | 16.5 ± 0.7 | 26 ± 3 | −[d] |
| 1($NO_2$) | 420 ± 80 | 78 ± 4 | 184 ± 29 | −[d] |
| 3(H) | 65800 ± 11000[c] | 387 ± 44[c] | 5.9 ± 0.4[c] | 21 ± 0.6[c] |
| 3($NO_2$) | −[d] | −[d] | −[d] | 324 ± 4[b] |

[a]Fitted with eq 4. [b]Slope of the linear fit. [c]Eq 4 + $k_I$[styrene]. [d]Predominant D or $I_a$ mechanism, the respective rate constant cannot be determined. DEDAM contains two double bonds per molecule.

reasonable, but with a view to the BuVE and 1-hexene experiments, a single activation pathway appears to be less likely. Since at realistic [DEDAM] the $k_{obs}$ values for DEDAM initiation have not reached the respective ceiling rates, it cannot be excluded that there is some contribution from $k_I$·[DEDAM]. However, the attempted fitting of the $k_{obs}$ vs [DEDAM] to (eq 4) + $k_I$·[DEDAM] does not converge to a well-defined set of parameters. To obtain an estimate of the potential involvement of an interchange mechanism in the DEDAM reactions, the dissociation rates $k_D$ for complexes **1** and **2** obtained from the $PCy_3$ initiation were used for a simplified fit procedure. This is based on the assumption that the $k_D$ based on $PCy_3$ for complexes **1** and **2** are primarily dissociative and thus independent from the nature of the substrate. This modified fit according to $k_{obs} = k_D(PCy_3)\cdot k_4/k_{-D}\cdot[\text{olefin}]/(1 + k_4/k_{-D}\cdot[\text{olefin}]) + (k_I\cdot[\text{olefin}])$ (eq 4) confirmed a largely dissociative pathway, except for a few of the electron-deficient complexes **1** and **2**, the interchange contribution appears to be negligible.

There is a large spread in the dissociative rate constant $k_D$ for complexes **1** which correlate well with the respective Hammett constants relative to the benzylidene carbon (Supporting Information, Figure SI-55). The initiation of complexes 3(H) and 3($NO_2$) with DEDAM and with styrene is much faster than that of complexes 1(H) and 1($NO_2$). Due to the modest curvature of the $k_{obs}$ vs [DEDAM] plots with complexes **3**, the hyperbola according to (eq 4) is less well-defined and a linear fit of the data more appropriate.

**Comparison of the Olefins.** In order to evaluate the substitution strength of the olefins utilized for the initiation reactions, the ratio of the respective $K_D\cdot k_4$ with the precatalysts 1($NEt_2$), 1(H) and 1($NO_2$) was calculated for BuVE and DEDAM. For identical ruthenium precatalysts, the values of $K_D$ should be identical, and consequently, the $K_D\cdot k_4$ ratio should reflect the ratio of $k_4$ (Scheme 5) for the two olefins. This step is important for the initiation reaction, but it is also closely related to the association of the olefin in the catalytic cycle of the actual olefin metathesis transformation. The analysis of $k_4$ should thus provide information on the ability of the respective olefin and the ruthenium complex to undergo olefin metathesis reactions. $K_D\cdot k_4$ is the initial slope of the $k_{obs}$ vs [olefin] plots and was determined via eq 4 (Table 6). Alternatively, at very low olefin concentrations the initiation reaction should be primarily dissociative, and then the ratio of the $k_{obs}$ can provide the same ratio of $k_4$. According to the two procedures, the following $k_4$(BuVE)/$k_4$(DEDAM) values were calculated (bracketed values are the respective ratios of $k_{obs}$ at [olefin] = 0.01 mol·L$^{-1}$): 1($NEt_2$) = 160 (177); 1(H) = 4 (6.5); and 1($NO_2$) = 1.3 (1.1). In general, BuVE attacks faster than DEDAM. For 1(H) the difference in olefin binding is significant, and for the electron-rich and poorly olefin binding complex 1($NEt_2$) the olefins are strongly differentiated, and the binding of more electron-rich olefin is preferred. The rapidly initiating and electron-deficient complex 1($NO_2$) hardly distinguishes between BuVE and DEDAM complexation in the initiation reaction. Since the propagating species in the limiting steps of the catalytic cycle of RCM reactions is of the Ru=$CH_2$ type,[55] the olefin binding capacity of the ruthenium species does not change. However, in cross metathesis reactions of electron-rich and electron-deficient olefins with different substitution strengths and different electron-densities of the resulting propagating ruthenium carbenes, the ratio of $k_4$ may well determine product distribution.

## SUMMARY AND CONCLUSIONS

The mechanism of the initiation reaction of electronically and sterically modified Grubbs−Hoveyda-type complexes with the olefins DEDAM, BuVE, 1-hexene, styrene, and neohexene was investigated. Based on the detailed analysis of the initiation kinetics, this reaction was shown to simultaneously follow two parallel pathways: a dissociative (D) mechanism and an interchange mechanism with associative mode of activation ($I_a$). The preference for one of the two possible modes of precatalyst activation critically depends on the steric and electronic properties of the respective ruthenium complexes and the olefin employed for the metathesis reaction:

(i) Electron-withdrawing groups at the benzylidene ether group of the Grubbs−Hoveyda complexes render an electron-deficient ruthenium and lead to an acceleration of both the interchange and the dissociative mechanism. Substituents at the 4-position of the benzylidene ether ligand (para to the benzylidene carbon) in complexes **1** exert a stronger effect on the initiation rates than


dx.doi.org/10.1021/ja208967h | J. Am. Chem.Soc. 2012, 134, 1104−1114

substituents in the 5-position (para to the ether oxygen) in complexes **2**.

(ii) Decreasing the steric bulk of the Grubbs–Hoveyda complexes, by replacing the 2-isopropoxy substituent in complexes **1** and **2** by a smaller 2-methoxy group in complexes **3**, leads to a pronounced acceleration of the olefin-dependent $I_a$ mechanism and consequently to a strong increase in the rate of precatalyst activation at high olefin concentrations.

(iii) Electron-rich and sterically less demanding olefins, such as 1-hexene or BuVE, prefer the $I_a$ activation. For the more bulky or less electron-rich olefins, such as DEDAM and styrene, the dissociative pathway is more important with bulky complexes **1** and **2**. With the less bulky complexes **3**, the olefin DEDAM undergoes precatalyst activation preferentially according to $I_a$, while styrene is a borderline case with comparable D and $I_a$ contributions.

In order to achieve rapid precatalyst initiation an electron-deficient and sterically accessible ruthenium is ideal, while the olefins should be electron-rich and sterically unhindered to promote both the dissociative as well as the interchange activation pathway. The combination of steric and electronic effects leads to Grubbs–Hoveyda-type complexes with widely differing rates of precatalyst activation. Complex **3**($NO_2$) with 4-$NO_2$ and 2-methoxy substituents initiates ca. 1000 times faster with DEDAM than precatalyst **1**($NEt_2$) with 4-$NEt_2$ and 2-isopropoxy substituents.

It remains to be shown in the future whether such a toolbox of catalysts with tunable initiation rates can be used for more efficient olefin metathesis transformations, by using precatalysts whose initiation rate is tailored to the needs of a specific substrate. Accepting the dual mechanism for precatalyst activation also helps to understand why different combinations of precatalysts and substrate lead to widely different reactivities in olefin metathesis reactions, despite the fact that the same catalytically active species is formed.

## ■ ASSOCIATED CONTENT

### Supporting Information

Experimental procedures for the synthesis of ligands and ruthenium complexes and characterization of complexes, copies of NMR and mass spectra, formal kinetics, Eyring plots, and cyclic voltammograms. This material is available free of charge via the Internet at http://pubs.acs.org.

## ■ AUTHOR INFORMATION

### Corresponding Author

plenio@tu-darmstadt.de

## ■ ACKNOWLEDGMENTS

We thank the DFG for support through grant Pl 178/8-3. We are grateful to Dr. X. Solans-Montfort for useful discussions and the Umicore AG for a donation of M31 complex.

## ■ REFERENCES

(1) Hoveyda, A. H.; Zhugralin, A. R. *Nature* **2007**, *450*, 243–251.

(2) (a) Leitgeb, A.; Wappel, J.; Slugovc, C. *Polymer* **2010**, *51*, 2927–2946. (b) Slugovc, C. *Macromol. Rapid Commun.* **2004**, *25*, 1283–1297. (c) Mutlu, H.; de Espinosa, L. M.; Meier, M. A. R. *Chem. Soc. Rev.* **2011**, *40*, 1404–1445. (d) Opper, K. L.; Wagener, K. B. *J. Polymer Sci. A* **2011**, *49*, 821–831.

(3) Nolan, S. P.; Clavier, H. *Chem. Soc. Rev.* **2010**, *39*, 3305–3316.

(4) Krische, M. J. *Proc. Nat. Acad. Sci.U.S.A.* **2010**, *107*, 3279–3280.

(5) (a) Hoveyda, A. H.; Malcolmson, S. J.; Meek, S. J.; Zhugralin, A. R. *Angew. Chem., Int. Ed.* **2010**, *49*, 34–44. (b) Fürstner, A. *Chem. Commun.* **2011**, *47*, 6505–6511.

(6) Meier, M. A. R. *Macromol. Chem. Phys.* **2009**, *210*, 1073–1079.

(7) Lin, Y. A.; Chalker, J. M.; Davis, B. G. *ChemBioChem* **2009**, *10*, 959–969.

(8) (a) Farina, V.; Shu, C.; Zeng, X.; Wei, X.; Han, Z.; Yee, N. K.; Senanayake, C. H. *Org. Process Res. Dev.* **2009**, *13*, 250–254. (b) Morzycki, J. W. *Steroids* **2011**, *76*, 949–966.

(9) Schrock, R. R. *Chem. Rev.* **2009**, *109*, 3211–3226.

(10) (a) Samojłowicz, C.; Bieniek, M.; Grela, K. *Chem. Rev.* **2009**, *109*, 3708–3742. (b) Vougioukalakis, G. C.; Grubbs, R. H. *Chem. Rev.* **2010**, *110*, 1746–1787.

(11) (a) Sanford, M. S.; Love, J. A.; Grubbs, R. H. *J. Am. Chem. Soc.* **2001**, *123*, 6543–6554. (b) Love, J. A.; Sanford, M. S.; Day, M. W.; Grubbs, R. H. *J. Am. Chem. Soc.* **2003**, *125*, 10103–10109.

(12) Louie, J.; Grubbs, R. H. *Angew. Chem., Int. Ed.* **2001**, *40*, 247–249.

(13) (a) Sashuk, V.; Peeck, L. H.; Plenio, H. *Chem.—Eur. J.* **2010**, *16*, 3983–3993. (b) Vorfalt, T.; Leuthäußer, S.; Plenio, H. *Angew. Chem., Int. Ed.* **2009**, *48*, 5191–5194. (c) Peeck, L. H.; Plenio, H. *Organometallics* **2010**, *29*, 2761–2768. (d) Bantreil, X.; Randall, R. A. M.; Slawin, A. M. Z.; Nolan, S. P. *Organometallics* **2010**, 29. (e) Wolf, S.; Plenio, H. *J. Organomet. Chem.* **2010**, *695*, 2418–2422.

(14) Romero, P. E.; Piers, W. E.; McDonald, R. *Angew. Chem.* **2004**, *116*, 6287–6291.

(15) (a) Romero, P. E.; Piers, W. E. *J. Am. Chem. Soc.* **2005**, *127*, 5032–5033. (b) Wenzel, A. G.; Grubbs, R. H. *J. Am. Chem. Soc.* **2007**, *128*, 16048–16049. (c) Romero, P. E.; Piers, W. E. *J. Am. Chem. Soc.* **2007**, *129*, 1968–1704. (d) van der Eide, E. F.; Romero, P. E.; Piers, W. E. *J. Am. Chem. Soc.* **2008**, *130*, 4485–4491. (e) Rowley, C. N.; van der Eide, E. F.; Piers, W. E.; Woo, T. K. *Organometallics* **2008**, *27*, 6043–6045. (f) Wenzel, A. G.; Blake, G.; VanderVelde, D. G.; Grubbs, R. H. *J. Am. Chem. Soc.* **2011**, *133*, 6429–6439. (g) vanderEide, E. F.; Piers, W. E. *Nat. Chem.* **2010**, *2*, 571–576.

(16) Bieniek, M.; Michrowska, A.; Usanov, D. L.; Grela, K. *Chem.—Eur. J.* **2008**, *14*, 806–818.

(17) (a) Diesendruck, C. E.; Tzur, E.; Lemcoff, N. G. *Eur. J. Inorg. Chem.* **2009**, 4185–4203. (b) Tzur, E.; Szadkowska, A.; Ben-Asuly, A.; Makal, A.; Goldberg, I.; Woźniak, K.; Grela, K.; Lemcoff, N. *Chem.—Eur. J.* **2010**, *16*, 8726–8737.

(18) (a) Michrowska, A.; Bujok, R.; Harutyunyan, S.; Sashuk, V.; Dolgonos, G.; Grela, K. *J. Am. Chem. Soc.* **2004**, *126*, 9318–9325. (b) Wakamatsu, H.; Blechert, S. *Angew. Chem., Int. Ed.* **2002**, *41*, 2401–2403. (c) Gułajski, Ł.; Michrowska, A.; Bujok, R.; Grela, K. *J. Mol. Cat. A* **2006**, *254*, 118–123. (d) Choi, T.-L.; Grubbs, R. H. *Angew. Chem., Int. Ed.* **2003**, *42*, 1743–1746.

(19) (a) Monsaert, S.; Vila, A. L.; Drozdzak, R.; Voort, P. V. D.; Verpoort, F. *Chem. Soc. Rev.* **2009**, *38*, 3360–3372. (b) Diesendruck, C. E.; Iliashevsky, O.; Ben-Asuly, A.; Goldberg, I.; Lemcoff, N. G. *Macromol. Symp.* **2010**, *293*, 33–38. (c) Ben-Asuly, A.; Tzur, E.; Diesendruck, C. E.; Sigalov, M.; Goldberg, I.; Lemcoff, N. G. *Organometallics* **2008**, *47*, 6422–6425. (d) Gstrein, X.; Burtscher, D.; Szadkowska, A.; Barbasiewicz, M.; Stelzer, F.; Grela, K.; Slugovc, C. *J. Polym. Sci., Part A* **2007**, *45*, 3494–3500. (e) Ung, T.; Hejl, A.; Grubbs, R. H.; Schrodi, Y. *Organometallics* **2004**, *23*, 5399–5401.

(20) (a) Kingsbury, J. S.; Harrity, J. P. A; Bonitatebus, P. J.; Hoveyda, A. H. *J. Am. Chem. Soc.* **1999**, *121* (-), 791–799. (b) Garber, S. B.; Kingsbury, J. S.; Gray, B. L.; Hoveyda, A. H. *J. Am. Chem. Soc.* **2000**, *122*, 8168–8179. (c) Gessler, S.; Randl, S.; Blechert, S. *Tetrahedron Lett.* **2000**, *41*, 9973–9976.

(21) Hoveyda, A. H.; Gillingham, D. G.; Veldhuizen, J. J. V.; Kataoka, O.; Garber, S. B.; Kingsbury, J. S.; Harrity, J. P. A *Org. Biomol. Chem.* **2004**, *2*, 8–23.

(22) Gatti, M.; Vieille-Petit, L.; Luan, X.; Mariz, R.; Drinkel, E.; Linden, A.; Dorta, R. *J. Am. Chem. Soc.* **2009**, *131*, 9498–9499.

(23) Kuhn, K. M.; Bourg, J.-B.; Chung, C. K.; Virgil, S. C.; Grubbs, R. H. *J. Am. Chem. Soc.* **2009**, *131*, 5313–5320.

(24) Monfette, S.; Fogg, D. E. *Chem. Rev.* **2009**, *109*, 3783–3816.

(25) (a) Vorfalt, T.; Wannowius, K. J.; Plenio, H. *Angew. Chem., Int. Ed.* **2010**, *49*, 5533−5536. (b) Vorfalt, T.; Wannowius, K.-J.; Thiel, V.; Plenio, H. *Chem.—Eur. J.* **2010**, *16*, 12312−12315.
(26) Zaja, M.; Connon, S. J.; Dunne, A. M.; Rivard, M.; Buschmann, N.; Jiricek, J.; Blechert, S. *Tetrahedron* **2003**, *59*, 6545−6558.
(27) (a) Grela, K.; Harutyunyan, S.; Michrowska, A. *Angew. Chem., Int. Ed.* **2002**, *41*, 4038−4040. (b) Bujok, R.; Bieniek, M.; Masnyk, M.; Michrowska, A.; Sarosiek, A.; Stepowska, H.; Arlt, D.; Grela, K. *J. Org. Chem.* **2004**, *69*, 6894−6896. (c) Bieniek, M.; Bujok, R.; Cabaj, M.; Lugan, N.; Lavigne, G.; Arlt, D.; Grela, K. *J. Am. Chem. Soc.* **2006**, *128*, 13652−13653. (d) Barbasiewicz, M.; Bieniek, M.; Michrowska, A.; Szadkowska, A.; Makal, A.; Wozniak, K.; Grela, K. *Adv. Synth. Catal.* **2007**, *349*, 193−203.
(28) Barbasiewicz, M.; Szadkowska, A.; Makal, A.; Jarzembska, K.; Wozniak, K.; Grela, K. *Chem.—Eur. J.* **2008**, *14*, 9330−9337.
(29) (a) Solans-Monfort, X.; Pleixats, R.; Sodupe, M. *Chem.—Eur. J.* **2010**, *16*, 7331−7343. (b) Nunez-Zarur, F.; Solans-Monfort, X.; Rodriguez-Santiago, L.; Pleixats, R.; Sodupe, M. *Chem.—Eur. J.* **2011**, *17*, 7506−7520.
(30) Vougioukalakis, G. C.; Grubbs, R. H. *Chem.—Eur. J.* **2008**, *14*, 7545−7556.
(31) Ashworth, I. W.; Hillier, I. H.; Nelson, D. J.; Percy, J. M.; Vincent, M. A. *Chem. Commun.* **2011**, 5428−5430.
(32) Süßner, M.; Plenio, H. *Angew. Chem., Int. Ed.* **2005**, *44*, 6885−6888.
(33) Hansch, C.; Leo, A.; Taft, R. W. *Chem. Rev.* **1991**, *91*, 165−195.
(34) Doppiu, A.; Winde, R.; Wörner, E.; Rivas-Nass, A.; Slugovc, C.; Lexer, C. Method for preparation of ruthenium-based metathesis catalyst with chelating alkylidene ligand. Patent WO 2010/127829, November 11, 2010.
(35) Complex **3**($NO_2$) contains a small amount (<5%) of the stilbene originating from the self-metathesis of 2-methoxy-4-nitrostyrene. Quantitive removal of the stilbene was not possible by chromatography due to the instability of this ruthenium complex.
(36) (a) Süßner, M.; Plenio, H. *Chem. Commun.* **2005**, 5417−5419. (b) Leuthäußer, S.; Schmidts, V.; Thiele, C. M.; Plenio, H. *Chem.—Eur. J.* **2008**, *14*, 5465−5481. (c) Collins, M. S.; Rosen, E. L.; Lynch, V. M.; Bielawski, C. W. *Organometallics* **2010**, *29*, 3047−3053. (d) Wolf, S.; Plenio, H. *J. Organomet. Chem.* **2009**, *694*, 1487−1492.
(37) Anslyn, E. V., Dougherty, D. A. Fitted according to the Yukawa-Tsuno equation. *Modern Physical Organic Chemistry*; University Science Books: Herndon, VA, 2006.
(38) The use of $\sigma+/\sigma-$ Hammett parameter for the substituents in the 4- and 5-position also leads to good correlations with the Ru(II/III) redox potentials.
(39) (a) Hansen, S. M.; Rominger, F.; Metz, M.; Hofmann, P. *Chem.—Eur. J.* **1999**, *5*, 557−566. (b) Getty, K.; Delgado-Jaime, M. U.; Kennepohl, P. *J. Am. Chem. Soc.* **2007**, *129*, 15774−15776.
(40) The need for a very large excess of olefin precluded kinetic studies using NMR spectroscopy.
(41) Higher DEDAM concentrations (up to 4 M) were also studied, but the $k_{obs}$ values at higher than 2.5 M cease to follow the hyperbolic function. It is important to know in this context that a 4 M DEDAM solution in toluene consists of 96% DEDAM and only 4% toluene.
(42) A 2 M DEDAM solution in toluene contains nearly 50% weight of the olefin. It might be argued that the change in the nature of the solution (dielectric constant) at very high olefin concentrations exerts a significant influence on the initiation behavior of the ruthenium complexes. We do not believe this effect to be of significance (at least up to 50% weight of olefin) based on the following arguments: (i) The higher dielectric constant of DEDAM compared to toluene might lead to an increase in the initiation rates. Instead a slowing down is observed; (ii) the $k_{obs}$ vs [olefin] plot for styrene and DEDAM are similar, even though concerning the dielectric constant the two olefins are very different; (iii) the strict linearity of $k_{obs}$ vs [olefin] observed for several initiation reactions with these and other olefins is hardly compatible with significant solvent effects; and (iv) different complexes lead to very different $k_{obs}$ vs [olefin] plots, for example, for related complexes **1** and **3** with the same olefin.
(43) Wilkins, R. G. *Kinetics and Mechanism of Reactions of Transition Metal Complexes*, 2nd ed.; VCH: Weinheim, Germany, 1991.
(44) Measurements at $PCy_3$ concentrations >0.3 M are less reliable due to increasingly important but unknown secondary reactions. The available data are not sufficient to resolve this issue, and hyperbolic data analysis was employed for all $PCy_3$ reactions.
(45) Adlhart, C.; Chen, P. *J. Am. Chem. Soc.* **2004**, *126*, 3496−3510.
(46) Bieniek, M.; Samojłowicz, C.; Sashuk, V.; Bujok, R.; Śledź, P.; Lugan, N. l.; Lavigne, G.; Arlt, D.; Grela, K. *Organometallics* **2011**, *30*, 4144−4158.
(47) (a) Anderson, D. R.; Hickstein, D. D.; O'Leary, D. J.; Grubbs, R. H. *J. Am. Chem. Soc.* **2006**, *128*, 8386−8387. (b) Stewart, I. C.; Benitez, D.; O'Leary, D. J.; Tkatchouk, E.; Day, M. W.; Goddard, W. A.; Grubbs, R. H. *J. Am. Chem. Soc.* **2009**, *131*, 1931−1938.
(48) Straub, B. F. *Adv. Synth. Catal.* **2007**, *349*, 204−214.
(49) Correa, A.; Cavallo, L. *J. Am. Chem. Soc.* **2006**, *128*, 13352−13353.
(50) (a) Alibrandi, G.; Bruno, G.; Lanza, S.; Minniti, D.; Romeo, R.; Tobe, M. L. *Inorg. Chem.* **1987**, *26*, 185−190. (b) vanEldik, R.; Hubbard, C. D. *Adv. Phys. Org. Chem.* **2006**, *41*, 1−78.
(51) Straub, B. F. *Angew. Chem., Int. Ed.* **2005**, *117*, 5974−5978.
(52) Occhipinti, G.; Bjørsvik, H.-R.; Jensen, V. R. *J. Am. Chem. Soc.* **2006**, *128*, 6952−6964.
(53) (a) Grela, K.; Kim, M. *Eur. J. Org. Chem.* **2003**, 963−966. (b) Krause, J. O.; Nuyken, O.; Buchmeiser, M. R. *Chem.—Eur. J.* **2004**, *10*, 2029−2035.
(54) Atkins, P. W. *Physikalische Chemie*; VCH: Weinheim, Germany, 1990.
(55) This concerns the intermolecular reaction with olefin and does not apply to the ring closing step with a bound alkylidene ligand. However, the intermolecular reaction with an olefin can be expected to be much faster than the corresponding intramolecular reaction.